Contribution of IASI to the observation of dust aerosol emissions (morning and nighttime) over the Sahara desert

Article (Published Version)

JGR Atmospheres

RESEARCH ARTICLE
10.1029/2019JD032014

Contribution of IASI to the Observation of Dust Aerosol Emissions (Morning and Nighttime) Over the Sahara Desert

A. Chédin[1], V. Capelle[1], N. A. Scott[1], and M. C. Todd[2]

[1]Laboratoire de Météorologie Dynamique, UMR8539, CNRS/IPSL, Ecole Polytechnique, Université Paris-Saclay, Palaiseau, France, [2]Department of Geography, University of Sussex, Brighton, UK

Key Points:

- Twelve years of IASI Saharan dust properties (AOD and altitude) are used to assess its capability to bring information on dust emission morning and nighttime
- Measuring at 0930 hr and 2130 hr local time, IASI is relatively well matched to the main Saharan dust uplift mechanisms
- Morning and nighttime dust emission is analyzed and compared to available results at both daily (Fennec campaign) and climatological scales

Correspondence to:
A. Chédin,
chedin@lmd.polytechnique.fr

Citation:
Chédin, A., Capelle, V., Scott, N. A., & Todd, M. C. (2020). Contribution of IASI to the observation of dust aerosol emissions (morning and nighttime) over the Sahara desert. *Journal of Geophysical Research: Atmospheres*, *125*, e2019JD032014. https://doi.org/10.1029/2019JD032014

Received 7 NOV 2019
Accepted 6 JUL 2020
Accepted article online 8 JUL 2020

Abstract Observing the planet at global scale, twice a day, and measuring the whole infrared atmospheric spectrum (8,461 channels at 0.50 cm^{-1} resolution), Infrared Atmospheric Sounder Interferometer (IASI)/METOP can concurrently detect clouds, determine the 3-D atmospheric structure (temperature, water vapor, ozone, etc.), surface properties (emissivity and temperature), as well as dust aerosol AOD and altitude. Observing morning (0930 hr) and nighttime (2130 hr), IASI is in relatively good phase with the most frequent times of occurrence of the main Saharan dust uplift mechanisms reported in the literature. Here we classify IASI dust observations according to both the dust loading (AOD) and the dust layer height, providing a more comprehensive picture of dust characteristics. This classification is analyzed at daily scale and its capability to detect dust uplift events is evaluated through comparisons with results from the particularly well documented June 2011 Fennec campaign. Then, a Dust Emission Index (DEI), specific to IASI, is constructed by selecting AOD-altitude bins with largest AODs and smallest altitudes likely indicative of freshly emitted dust. Applying this to the 12-year 2007–2018 period, we determine climatological DEI maps and comparisons are made with other equivalent existing results derived from ground-based or other satellite observations. Results of these comparisons demonstrate the capability of IASI to document the dust distribution over the whole Earth desert areas over a long period of time. The present approach is also suitable to the processing of the at least hourly observations of the coming Infrared Sounder instrument (IRS), planned on board Meteosat Third Generation (2021).

1. Introduction

Aerosols, originating from either natural or anthropogenic sources, play an important role in the Earth's climate. In suspension in the atmosphere, these particles impact the Earth's radiative budget, directly by interacting with solar and terrestrial radiation, and indirectly through their interaction with cloud properties and other components of the atmosphere or oceanic and terrestrial biogeochemical cycles. Their highly variable spatial and temporal distribution makes their study complex, and aerosols continue to contribute one of the largest uncertainties to the total radiative forcing estimate (Boucher et al., 2013). Indeed, a recent study by Kok et al. (2017) raises the possibility that dust causes a net warming of the planet. More fully understanding the climate impact of dust requires more accurate information on their space/time distribution, including their diurnal cycle and identifying dust source regions, to help validation of climate-aerosol model simulations.

The Infrared Atmospheric Sounder Interferometer (IASI), on board the suite of European Satellites METOP, is particularly well suited to accurate monitoring of dust characteristics (Callewaert et al., 2019; Capelle et al., 2014, 2018; Chedin et al., 2018; Clarisse et al., 2019; Cuesta et al., 2015; Klüser et al., 2011, 2012; Peyridieu et al., 2010, 2013; Pierangelo et al., 2004). IASI provides, at global scale, unique simultaneous information on Aerosol Optical Depth in the infrared, dust layer altitude, as well as surface temperature. In addition, clouds are accurately detected and well distinguished from the aerosols. A long time series of IASI data is being constructed with the launch of the platforms METOP A, B, and C in, respectively, October 2006, September 2012, and November 2018. IASI exhibits excellent calibration and stability as well as showing equal quality performance (noise) from daytime and nighttime observations (Hewison et al., 2013). The IASI observation times, with local equatorial crossing times in the morning at 0930 hr LT and nighttime at 2130 hr LT, match relatively well the times of occurrence of the two dominant dust uplift mechanisms,

at least over the Sahara desert: (1) the breakdown of the nocturnal low-level jet (NLLJ), which drives dust emissions peaking in the midmorning when the LLJ momentum is mixed to the surface after sunrise (Allen et al., 2013; Allen & Washington, 2014; Blackadar, 1957; Heinold et al., 2013; Holton, 1967; Knippertz et al., 2007; Marsham et al., 2011; Marsham, Dixon, et al., 2013; Parker et al., 2005; Schepanski et al., 2009; Todd et al., 2008, 2013; Washington & Todd, 2005; Washington et al., 2006, 2009); (2) density currents, or cold pools, occurring when downdraughts in moist convective systems spread out at the surface whose strong winds generate dust fronts (haboobs) (Allen et al., 2013; Allen & Washington, 2014; Flamant et al., 2007; Knippertz & Todd, 2010, 2012; Marsham et al., 2008; Roberts & Knippertz, 2012; Williams et al., 2009). Cold pools tend to occur preferentially in the afternoon hours but may also occur during a large diurnal window (Allen & Washington, 2014; Emmel et al., 2010; Flamant et al., 2009; Heinold et al., 2013; Knippertz et al., 2007; Knippertz & Todd, 2012; Liu et al., 2018; Marsham et al., 2011; Marsham, Dixon, et al., 2013; Pantillon et al., 2016; Roberts et al., 2018; Schepanski et al., 2009; Vizy & Cook, 2018). Dust emissions over the Sahara have been the subject of many studies over the last years and are now relatively well known: see Knippertz and Todd (2012) for a comprehensive review.

The aims of this paper are as follows:

1. To assess the capability of IASI-derived AOD-altitude bins to detect dust emission events. This is done at daily scale, morning and nighttime;
2. Help locate dust emission sources morning and nighttime, bringing an important piece of information for model validation. This is done at climatological scale (2007–2018).

Research aim (1) involves analyzing, at daily scale, morning and nighttime, dust AOD-altitude bins for situations selected from the particularly well documented June 2011 Fennec campaign (Washington et al., 2012). To address aim (2) we construct a Dust Emission Index (DEI) specific to IASI, based on the selection of "high AOD-low altitude" bins. This simultaneous information on AOD and altitude, unique to infrared sounders such as IASI, allows discriminating between aged higher-level transported dust and lower-level dust plumes emitted recently by dust sources. Comparisons are done between the 12-year DEI monthly climatology and other equivalent existing results over the Sahara.

2. Determination of Dust AOD and Altitude From IASI Observations

2.1. IASI Instrument

IASI, developed by the Centre National d'Etudes Spatiales (CNES) in collaboration with the European Organization for the Exploitation of Meteorological Satellites (EUMETSAT), is a Fourier transform spectrometer based on a Michelson interferometer that measures infrared radiation emitted from the Earth. IASI provides 8,461 spectral channels covering the interval between 645.00 and 2,760.00 cm^{-1} (15.5 and 3.63 μm), with a high spectral resolution of 0.50 cm^{-1} after apodization and a spectral sampling interval of 0.25 cm^{-1}. IASI provides a near global coverage with an instantaneous field of view (grid cell pixel) of 12 km at nadir. IASI is designed to fly on board the METOP series of three polar orbiting meteorological satellites (METOP A, B, C). METOP-A, whose data are used in the present study, was launched in October 2006 and we use Level-1C data from July 2007 until December 2018. With 14 orbits (swath width of 2,200 km), a global coverage can be provided twice a day with a local equatorial crossing times in the morning at 0930 hr and nighttime at 2130 hr local time.

2.2. Determination of Dust AOD and Altitude

The method used to derive dust layer AOD and mean altitude from IASI observations is detailed in Capelle et al. (2018) (see also Capelle et al., 2014; Chedin et al., 2018; Peyridieu et al., 2010, 2013; Pierangelo et al., 2004, 2005). It is based on a physical approach relying on the use of Look-up-Tables (LUTs) of simulated IASI cloud-free brightness temperatures computed for a large selection of atmospheric situations, for extended ranges of variation of surface properties (spectral emissivity, temperature, and pressure), as well as of dust optical characteristics. It is worth pointing out that, due to its high spectral resolution, IASI offers channels which are sensitive to very specific atmospheric or surface variables without being significantly "polluted" by other variables. For example, some channels are much more sensitive to the atmospheric temperature close to the surface than to the surface itself (channel n°6254 at 4.52 μm, whose peak sensitivity is at 930 hPa, has a top-to-surface atmospheric transmission of 0.11).

Each IASI cloud-free observation is interpreted with respect to the brightness temperature LUTs in terms of dust optical properties (AOD and altitude) and surface temperature. If the concept of AOD is familiar, it is less the case of the altitude as derived from an infrared vertical sounder like IASI. As recalled in Capelle et al. (2018), the IASI dust layer altitude represents the median of the dust layer: it corresponds to the altitude at which half of the dust optical depth is below and half of the optical depth is above and can be considered as an infrared optical equivalent to the centroid of the real vertical profile. Only cloud-free situations are used in this study. This requires making the distinction between cloudy and dusty pixels. Here the cloud mask relies on nine screening tests combining the infrared IASI observations and collocated observations from the AMSUA (Advanced Microwave Sounding Unit), much less sensitive to clouds, also on board the METOP platform: six tests to detect high, medium, and low clouds and three tests dedicated to the discrimination between clouds and aerosols (see Capelle et al., 2018; Pernin et al., 2013 for details). All tests use threshold values which depend on the season, viewing angle, surface emissivity and are computed separately for night and day conditions.

Retrieval of aerosol properties over land surfaces, and specifically over arid and desert regions, is more difficult than over ocean surfaces due to the large variability of the surface emissivity. Emissivity data used here are from Capelle et al. (2012) recently enhanced to provide 0.5° gridded data instead of the original 1° resolution in order to comply with the resolution defined for the present study. Emissivity spectra cover the whole IASI spectral range at a resolution of 0.05 μm.

Since 2004, extensive validations of Atmospheric Infrared Sounder (AIRS) and then IASI-retrieved dust characteristics (AOD and altitude) have been presented (Capelle et al. 2014; Peyridieu et al., 2010, 2013; Pierangelo et al., 2004) based on comparisons against a variety of data sources: Moderate Resolution Imaging Spectroradiometer (MODIS), Polarization and Anisotropy of Reflectances for Atmospheric Science coupled with Observations from a Lidar (PARASOL), Multiangle Imaging Spectroradiometer (MISR) for the AOD, Cloud-Aerosol Lidar with Orthogonal Polarization (CALIOP) for the altitude. More recently, Capelle et al. (2018) have compared daily-scale IASI-retrieved AODs to data from 80 ground-based AErosol RObotic NETwork (AERONET) sites well distributed within the "dust belt" (Sahara, Arabian Peninsula, Mediterranean basin, India, and also the Caribbean). Results, covering the time period extending from July 2007 to December 2016, show an overall correlation of 0.8 between the two products. This may be considered satisfactory especially given uncertainties associated with the necessary conversion of the AOD from infrared to visible. In the same study, spatial distributions of AOD have also been compared to MODIS/TERRA and Spinning Enhanced Visible and Infrared Imager (SEVIRI), showing a strong consistency. Still at daily scale, IASI altitudes have been compared with CALIOP mean altitudes (Kylling et al., 2018). Comparisons with CALIOP are not easy to interpret, given the different characteristics of the two instruments: much higher vertical resolution of CALIOP (IASI provides information on the atmospheric vertical structure with a resolution of ~1 km in the lower troposphere to 2 km in the free troposphere, Chalon et al., 2001; see also the iasi.cnes.fr/en and https://www.eumetsat.int websites), observation times differing by about 4 hr, difference in the altitude definition, difference in the spatial resolution, low CALIOP repeat cycle of 16 days, lower CALIOP daytime signal-to-noise ratio. Nevertheless, these comparisons have demonstrated the capability of IASI altitudes to, at least, categorize the aerosol layer observed into low, medium, or high altitude. Recently, IASI data have been used to detect dust AOD trends over Sahara (Chedin et al., 2018) and to quantify African dust deposition along the trans-Atlantic transit (Yu et al., 2019).

For the present study, gridded IASI dust characteristics time series are constructed. To do so, daily IASI data, AOD and altitude at the pixel resolution, are first gridded at 0.5° in latitude and longitude. This is done separately for morning and nighttime satellite overpasses. Then, for each grid cell, monthly medians (preferred to the more classic mean given the often nonnormal distribution of daily data) are computed for each of the 144 months of the period ranging from July 2007 to December 2018 analyzed here.

2.3. Problem of the Cloud Mask

Due to the lack of surface observations, in particular over Sahara, satellite data represent the primary source of information. However, the inability of infrared or visible sounders to make observations under cloudy areas represents the most serious limitation of this type of instruments. Observing LLJ events should not be too big a problem for space observations as they mostly appear under clear-sky conditions (Schepanski et al., 2009). This is not the case of haboobs often associated with the presence of clouds in Multi

Convective Systems (MCS). This difficulty may lead to a so-called "morning bias" in the daily analysis of dust uplift events (if not normalized, contrary to the DEI) (Heinold et al., 2013; Marsham et al., 2011; Schepanski et al., 2007, 2012; Tegen et al., 2013). If this limitation may be real at the daily scale, it is less a problem at the monthly scale, and a fortiori at the climatological scale, as observations are often possible at the haboob leading edge (Knippertz et al., 2007; Marsham et al., 2008; Todd & Cavazos-Guerra, 2016, hereafter TCG16).

3. From Dust Characteristics (AOD and Altitude) to the IASI DEI

Determining dust source locations is of major concern for an improved comprehension of the origin and subsequent dispersion of dust over the planet. Satellite observations providing global coverage are an essential tool for such a study. However, several difficulties in identifying surface emission sources, inherent to these approaches, have been identified (Ashpole & Washington, 2012, 2013; Harrison et al., 2019; Heinold et al., 2013; Marsham et al., 2011; Schepanski et al., 2007, 2012; TCG16; Tegen et al., 2013). These include distinguishing dust from cloud and "bright" desert surfaces, or fresh emission from aged transported dust; identifying dust over the pronounced diurnal cycle: especially problematic may be a robust observation of dust at night for instruments measuring in the visible, or even for infrared instruments when too few channels are available to deal with the reduced surface-dust temperature contrast. In the present approach, we use the features of IASI to address these challenges. The possibility offered by IASI to combine dust AOD and altitude allows the categorization of each into a single variable combining the two basic properties. Here we categorize each AOD value and each altitude value as being "low," "medium," or "high" using predetermined threshold values. For AOD, the three categories correspond to 0.25–0.5 (low: designated by the symbol "L"), 0.5–0.8 (medium: "M"), >0.8 (high, "H"); for altitude, the three categories correspond to 0.0–1.1 (low), 1.1–2.1 (medium), 2.1–4.0 (high) in kilometer (note that infrared AOD values given here are about half of their values in the visible range, Capelle et al., 2014). Then, nine classes can be defined by two letters, the first referring to altitude the second to AOD, e.g., HH, meaning high altitude and AOD; HM, high altitude and medium AOD; HL, high altitude and low AOD; etc. Selecting bins with lower altitudes and higher AODs thus appears as a way to identify surface dust emission. If the "LH" class appears the most adapted to such an identification, classes "LM" and, to a lesser extent, "LL" may also correspond to surface dust events of smaller intensity. Conversely, bins with higher altitudes and smaller AODs are more likely to characterize transport. NB: observations with AOD < 0.25 are not categorized because it is assumed that they are not associated with fresh dust emission.

3.1. Daily-Scale Analysis of Dust AOD-Altitude Bins: Application to the Fennec Project Intensive Observation Period June 2011

We assess this new AOD-altitude classification for selected cases during the Fennec IOP in June 2011, which have been particularly well documented (Washington et al., 2012, notably at the supersite of Bordj-Badji Mokhtar in the extreme south of Algeria; BBM, 21.38°N, 0.92°E, close to the Algeria-Mali border). This is done daily, for morning and nighttime observations separately, at the IASI pixel resolution (12 km at nadir). Figure 1 shows results for the 17 June 2011: morning (left) and nighttime (right); AOD (top), altitude (middle), AOD-altitude bins (classes) (bottom). On this Figure, we first note the successive IASI orbits, here limited to a viewing angle of ±50° around the subsatellite track (Capelle et al., 2018) leaving holes in between (the present availability of IASI on board the METOP-B and METOP-C platforms could partly reduce this limitation intrinsic to polar orbiting satellites at low latitudes).

The 17th June 2011 case over the Western Sahara is highly instructive in that a particularly complex set of dust emission mechanisms and subsequent transport are apparent, which serve to demonstrate the capabilities of IASI, as well as the limitations. Concerning the evening overpass (exact observation time at BBM: 2115 hr), the main low altitude and high AOD (LH) dust feature observed is located in northern Mali immediately southwest of BBM (Feature A) at ~19°N, 0°E. This feature is surrounded by MH classes, characterized by medium altitudes and strong AOD (>0.8), which we infer is the dust emitted and transported over previous evening and morning (see analysis of the morning IASI pass below). This is consistent with our understanding of the complex sequence of emission and transport in this area around the triple point border of Mali-Algeria and Niger. Allen et al. (2013) document three cold pool events on the 17th June successively crossing the BBM supersite, at 0600 (observed in the morning IASI overpass, see below), 1700, and 2140 hr. They all have a long duration (~10 hr). The two afternoon haboobs are generated by a MCS

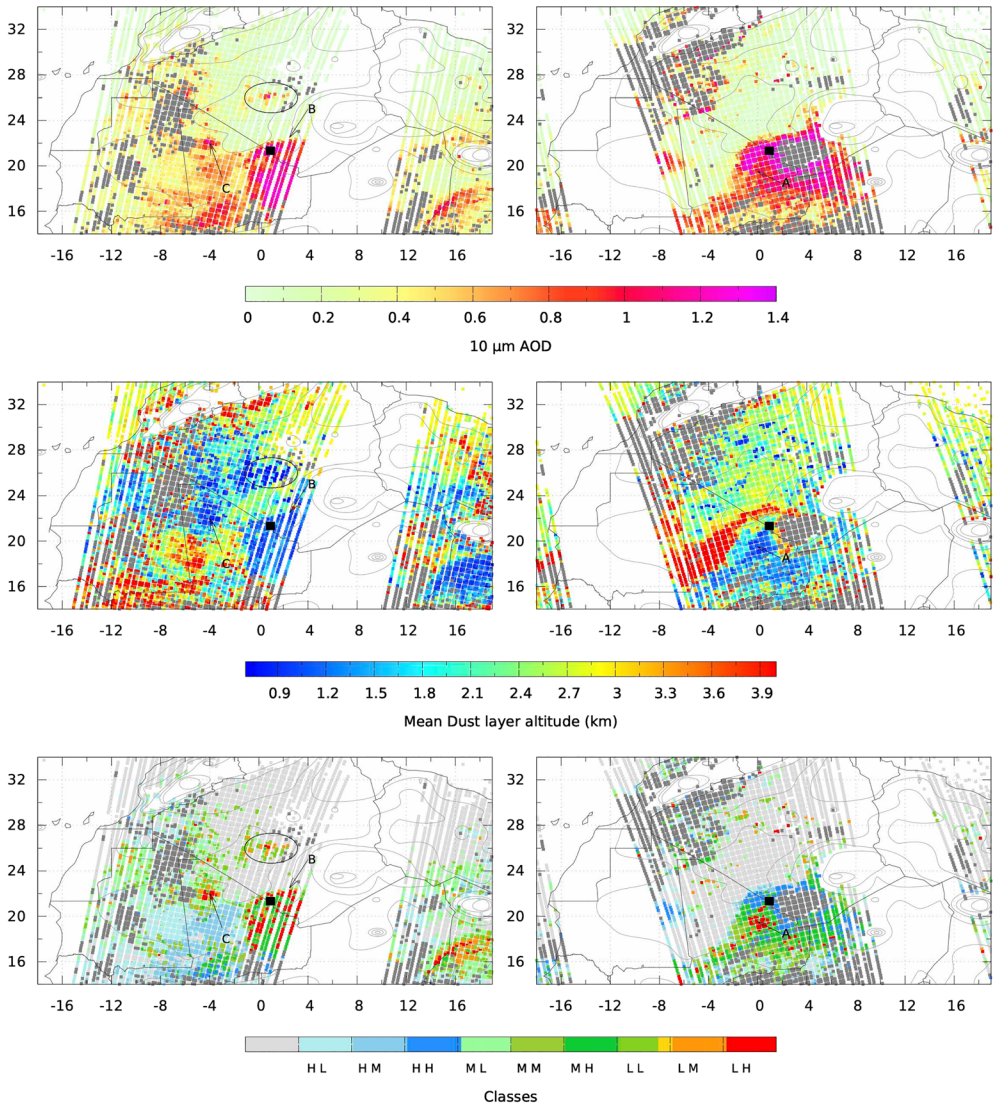

Figure 1. IASI results for the 17th June 2011 at 0930 hr (left) and 2130 hr (right); AOD (top), altitude (middle), AOD-altitude classes (bottom; see text). Dark gray applies for clouds detected by IASI; light gray applies for classes out of the range of the AOD-altitude classes defined in the text (section 3). Black square = BBM location; features A, B, C and the black contour = see text.

located to the south west of the Hoggar mountains to the northeast of BBM (identified as cloud covered pixels, in dark gray on Figure 1, right panels) and which then propagate southwestward into northern Mali and involve active emission over BBM (Allen et al., 2013). By the 2115 hr IASI pass this fresh emission is apparent as LH clearly showing the ability of IASI to distinguish the fresh emission from more aged dust and highlights dust emission inferred from the low dust layer altitude during the nighttime pass resulting from active haboob events. Note that the haboob dust emission event observed at BBM at 1700 hr cannot be directly observed by IASI.

For the morning overpass, the largest feature observed in the AOD-altitude classes is located around BBM, where the "LH" class (i.e., low altitude and high AOD, in red) is seen principally north of BBM (Feature B) whereas a mix of the "LH" and "MH" (medium altitude and high AOD in green) classes is observed south of BBM. At this precise location, the exact observation time is 1000 hr, slightly different from the equatorial crossing time. North of BBM, this feature B is also characterized by a sharp transition between the "LH" class and the "light-gray" class corresponding to the absence of strong dust event. Allen et al. (2013) identified a cold pool, arriving at BBM at about 0600 hr, generated the evening before by a convective system located

southeast of the Algeria-Mali-Niger triple point and propagating radially northwestward. Low altitudes close to BBM as well as slightly higher altitudes southward are consistent with lidar observations as reported in Allen et al. (2013). In this particular case however, as noted in Allen et al. (2013), local wind speeds at BBM are low, implying that the dust is advected and not locally emitted. In northern Mali, another feature is characterized by the "LH" class (Feature C, centered on ~22°N, 4°W, over the known dust source of the Taoudenni paleo lake deposits). It has been directly observed during the Fennec research aircraft flight b600 at 1000 hr (Ryder et al., 2015) and identified as a LLJ emission event caused by strong northeasterly winds. The dust layer, characterized by exceptionally large particle size, has been located below 1,400 m. These strong winds generated a series of LLJs driving dust propagation southwestward (Harrison et al., 2019). They are identified by IASI, either by the "LH" class (26°N, 1°E, dark contour) or other low altitude classes ("LM" and "LL") corresponding to smaller AOD, but all larger than an equivalent of 0.5 in the visible.

The morning IASI pass, while showing the utility of the IASI dust altitude, illustrates some of the challenges in inferring dust emission: First, that overnight dust can be transported considerable distances while remaining close to the surface, introducing some uncertainty into the dust emission inference. Second, that haboob events can occur over a broad time window including as late as the morning following nocturnal convection (Roberts & Knippertz, 2014). As such while the nighttime pass will not record LLJ dust emission the morning pass can include LLJ and haboob emission.

Visual comparisons between IASI results and in situ or other satellite observations (essentially from SEVIRI) from the whole Fennec campaign in general lead to a satisfactory agreement (Gonzalez & Briottet, 2017). Results for June 2011 are available upon request to the authors.

Several important remarks come from this limited comparison. First, by estimating both the height and concentration of the dust aerosol plumes, our processing of IASI AOD-altitude product provides an entirely new perspective of dust characteristics allowing to distinguish likely fresh emission from aged dust. Further, dust height has an important bearing on dust radiative effect, especially in the longwave. However, delivering only two "snapshots" of the situation per day, IASI obviously misses dust uplift events. Moreover, these events may be observed after their real "birth." Compared to the very high temporal resolution of SEVIRI, which allows "back-tracking" dust events (Ashpole & Washington, 2012, 2013; Schepanski et al., 2009, 2012), its main advantages are stable daytime/nighttime observations, combined AOD/altitude observations, planned long record, and a global coverage. As with any instrument, the advantages must be weighed against the disadvantages (a recognition that also applies to SEVIRI). Actually, the present IASI two snapshots instrument results have to be considered as a preliminary training phase for application to the at least hourly observations of the coming similar Infrared Sounder instrument (IRS), planned on board Meteosat Third Generation (2021).

3.2. The IASI Climatological (2007–2018) DEI

Characterizing dust emission from long-term space observations implies locating surface dust sources potentially active at the time of the satellite overpass. If, as seen above, IASI misses dust events at daily scale, observations cumulated over a long period of time should enhance the most active dust sources provided the timing of the two IASI overpasses approximately corresponds to the preferential times of occurrence of the main dust uplift mechanisms observed over Sahara, which is the case. The IASI instrument offers capabilities that substantially address a number of challenges faced by dust sources identification. (1) A good discrimination between clouds and dust; (2) observing in the infrared, there is no confusion with "bright" surfaces, and nighttime observations noise is similar to that of daytime ones; (3) the simultaneous knowledge of AOD and altitude helps distinguishing low-level recently emitted dust from higher-level transported aged dust.

We here construct the climatological DEI specific to IASI by binning simultaneous information on the dust layer AOD and its altitude. To do so, for each day of the whole time period analyzed, grid points characterized by a high 10 μm AOD, larger or equal to 0.5 (equivalent to an AOD of about 1.0 in the visible), and a low dust layer mean altitude (≤1.1 km asl) are first selected, corresponding to the two "LH" and "LM" classes defined in section 3. Thus defined, the DEI is compatible with the few existing observations, mostly from the June 2011 Fennec campaign. Indeed, for morning (typically LLJ) as well as for evening (often haboob type) an altitude of ~0.6–0.8 km at the time of the peak emission is observed (Allen et al., 2013; Marsham, Hobby, et al., 2013, TCG16). During the summer months, especially over the Sahara after emission, dust

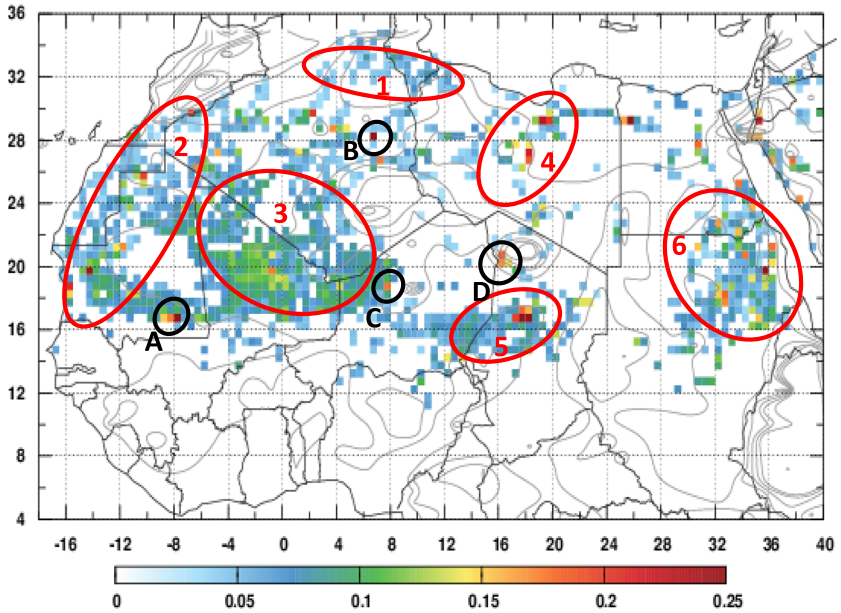

Figure 2. IASI 0.5° resolution Dust Emission Index for the whole period July 2007 to December 2018, morning and nighttime. The red contours delineate approximately the six regions identified on Figure 1 of Formenti et al. (2011). The black contours delineate small features discussed in the text.

is very rapidly mixed vertically through the deep boundary layer (Marsham, Hobby, et al., 2013) such that the DEI condition of mean dust altitude ≤1.1 km should indicate freshly emitted dust, although we must be aware of the uncertainty associated with transport in the shallow nighttime boundary as noted above. Frequency of occurrence of such emission grid points are then determined for mean monthly, seasonal, and annual values over the 12-year period. Finally, the DEI is defined as the resulting grid point frequency of occurrence, normalized by the number of cases observed (clear sky, with or without dust). Results are presented either separating 0930 hr from 2130 hr results or by regrouping all data.

4. Results and Discussion

4.1. IASI DEI Maps Over Sahara

Figure 2 shows the IASI-DEI over Sahara for the whole 12-year period of time analyzed, morning plus nighttime. To qualitatively evaluate the DEI results we compare them to a synthesis of previous dust source analyses (e.g., Formenti et al., 2011, 2014; Ginoux et al., 2012; Scheuvens et al., 2013, Weinzierl et al., 2017). In such studies, dust sources are identified using various complementary data including ground-based visibility data, analysis of chemical/mineralogical composition of the aerosol and underlying soil, and satellite observations in which dust sources can be inferred from either dust plume back trajectories from high frequency SEVIRI data (Ashpole & Washington, 2012, 2013; Schepanski et al., 2007, 2009, 2012) or frequency-type analysis (Ginoux et al., 2012, TCG16). In particular, Formenti et al. (2011) locate six major potential source areas (see their Figure 1): (1) northern Algeria and Tunisia, (2) southern Atlas and western Sahara-Mauritania, (3) Mali-Algerian border, (4) central Lybia, (5) Chad Bodele paleo lake, and (6) southern Egypt-northern Sudan. It can be noted that most of these dust source regions correspond to alluvial deposit or paleolakes geomorphic regions (see Bakker et al., 2019; Damnati, 2000; and Figure 3 of Lézine et al., 2014). These areas are identified (red contours) on Figure 2 showing the good general match between IASI results and this compilation of independent results. Of particular importance in the IASI DEI are large regions of high dust emission: southwestern Algeria-northern Mali, Algeria-Mali-Niger triple point (together they constitute region 3 in Formenti et al., 2011), Bodele Depression, central Mauritania, northern Sudan, for which the agreement with the above studies is satisfactory.

In addition to these broad-scale dominant source regions, more localized DEI maxima (black circles) on Figure 2 show good correspondence with previously listed dust sources: (A) the relatively small feature

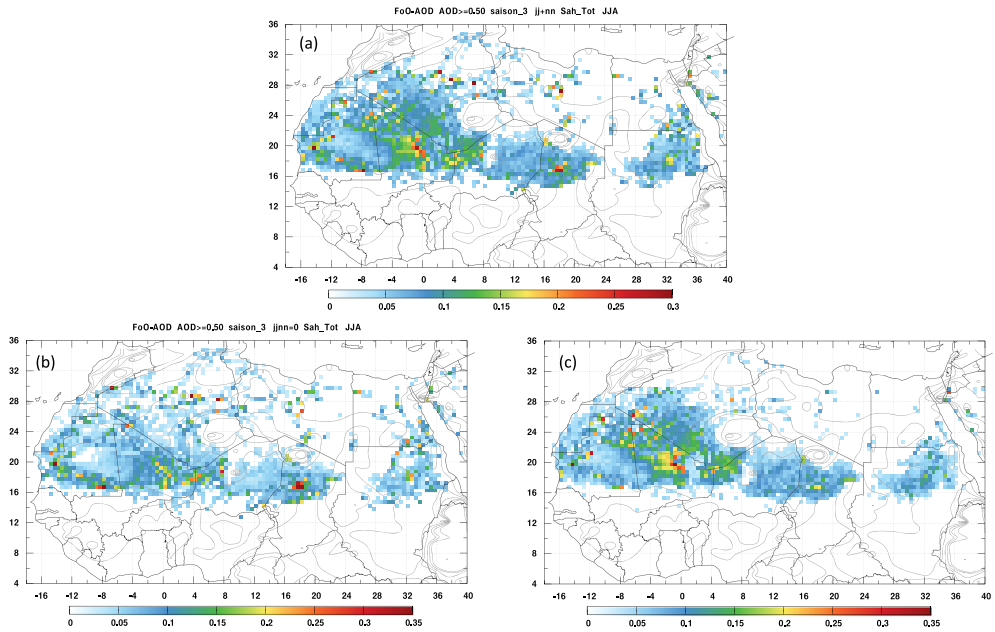

Figure 3. Maps of the IASI-DEI in summer (June to August) for the time period 2007–2018; (a) morning (0930 LT) plus nighttime (2130 LT), (b) nighttime, (c) morning.

near the southern border of Mauritania, close to 8°W–17°N, within the Aoukar depression, which is also well identified in Weinzierl et al. (2017) during the campaigns SAMUM (Ansmann et al., 2011; Formenti et al., 2011; see also Heintzenberg, 2009) and SALTRACE (Groß et al., 2016); (B) the feature seen around 7°E–28°N within the Great Oriental Erg and also identified during SALTRACE (see Weinzierl et al., 2017); (C) the small feature west of the Aïr massif, around 8°E–18°N also discussed in TCG16 and in the recent paper by Feuerstein and Schepanski (2019); (D) the small feature west of the Tibesti massif near 16°E–20°N also present in Weinzierl et al. (2017) during the three above mentioned campaigns (winter and summer). Other such examples of good correspondence between source location compilations and IASI results can be seen in Caquineau et al. (2002) or Cowie et al. (2014). As a whole, Figure 2 and these more local matches give good confidence in the capability of the IASI climatological DEI to identify Saharan dust sources.

4.2. IASI DEI Morning and Nighttime Maps Over Sahara in Summer

Summer (June to August) is the dust emission peak season over the central-west Sahara (broadly zones 2 and 3 in Figure 2) (Engelstaedter et al., 2006; Marsham et al., 2011). Figure 3a shows the IASI-DEI over Sahara for summer (morning plus nighttime) which displays similarities with Figure 2 (whole time period), confirming the dominant role of this season. Strong values of the IASI-DEI are seen in the border regions of southern Algeria, northern Mali, and northwest Niger, as well as for the Bodele Depression. These hotspots of dust emission match remarkably well with previous independent satellite analyses, including Schepanski et al. (2007), TCG16, and Ashpole and Washington (2013). The latter colocated many of these local dust hotpots with surface features such as paleolakes and outwash plains on the peripheries of mountains (their Figure 5 and Table 1). As such robust evidence based on the interaction of surface geomorphic features and dust emitting winds is being established and strengthened with our analysis of IASI data.

Important differences are observed between morning and nighttime IASI-DEI (Figures 3b and 3c, respectively) in response to the varying meteorological conditions, leading to different dominant dust uplift mechanisms. In our interpretation below we adopt a broad framework that emission from LLJs occurs essentially in the morning, while convective cold pools occur preferentially during the afternoon and nighttime (supported by, e.g., Marsham, Dixon, et al., 2013; see section 1). However, we must stress that this separation of emission mechanisms in time is not absolute and while the morning LLJ dust emission is strongly phase-locked to the diurnal cycle, haboob emission is less, so as evidenced by both high-resolution model

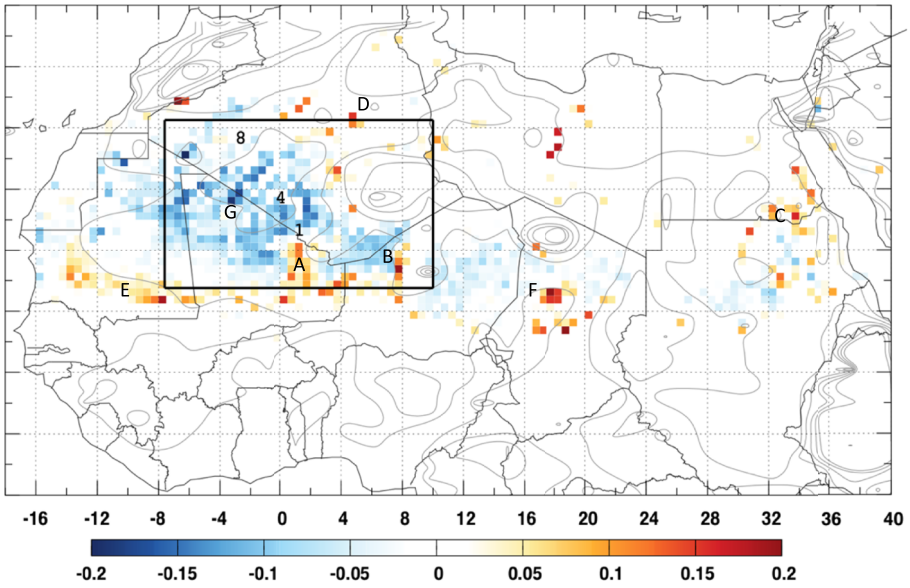

Figure 4. Difference between nighttime and morning IASI DEI for the summer season (June to August). The black rectangle delineates the Central West Sahara (CWS) region analyzed in Ashpole and Washington (2013) (see below). Labels 1, 4, and 8 locate the Fennec campaign sites F-101, F-134, F-138, respectively. Symbols "A" to "G" are discussed in the text.

results (Heinold et al., 2013) and surface observations: Allen et al. (2013) detect cold pools at Bordj Badji Mokhtar (shown on Figure 1 and as site 1 on Figure 4) on several mornings in June 2011, e.g., the morning of 17 June (Figure 1, left column).

Figure 4 shows the difference, computed from original daily data, between nighttime and morning IASI-DEI (Figures 3b and 3c, respectively). To understand the spatial pattern of these differences in DEI shown in Figure 4, we first undertake a comparison with other analyses of satellite data capable of resolving the diurnal cycle and then compare DEI to surface observation at specific locations in the Sahara.

DEI diurnal differences (Figure 4) can be compared to Figure 8c of TCG16 which presents analogous results using the aerosol characteristics provided by CALIOP for the period 2006–2013.

Comparing the two products must, however, take into account the differences existing between the two sounders: see section 2.2. Despite these differences, similar significant features may be seen on Figure 4 and, in particular, those indicating nighttime DEIs larger than the morning ones (red colors in Figure 4). This is the case for the regions of central-east Mali, the regions west of the Aïr massif, and southern Egypt-northern Sudan (Figure 4, features A–C, respectively). This is also the case at the northern and southern fringes of the desert (Figure 4, features D and E, respectively), consistent with the observations that haboobs are frequently observed there in the evening (Flamant et al., 2007; Knippertz et al., 2007; Marsham et al., 2011). This is as well the case of the Bodele depression (Figure 4, feature F) where large nighttime minus morning DEI differences are observed. Conversely, DEI is larger in the morning than in the nighttime for large areas of northern Mauritania and Mali and southern Algeria (blue-colored feature G in Figure 4), suggesting that LLJs are the dominant uplift mechanism. Findings of Ashpole and Washington (2013) allow making further inferences on the spatial structure of DEI diurnal differences. They analyzed SEVIRI observations over the Central West Sahara region (shown by the black rectangle on Figure 4) using an automated tracking method (see their Figure 10), and their findings appear to corroborate our results. They find that this region includes two broad areas. First, over southwest Algeria and northwest Mali (roughly centered on feature G in Figure 4) southwestward dust plume trajectories are observed with dust emission presumably dominated by LLJs embedded in the Harmattan. This region coincides with locations where morning DEI exceeds nighttime DEI (blue shades in Figure 4 around feature G). Conversely, over southern Algeria, northwest Niger, and northeast Mali, plume trajectories are much more variable and plumes are more proximate to deep convection suggesting associated cold pool outflows as the

dominant dust uplift mechanism. This region broadly coincides with locations where nighttime DEI exceeds morning DEI (red shades in Figure 4 around features A and B), although we must stress again, as Figure 1 shows, that the morning DEI is likely to reflect both LLJ emission and haboob emission/transport overnight.

The broad structure of DEI diurnal differences (Figure 4) is consistent with the observation that large horizontal pressure gradients, existing around the summer Saharan heat low, enhance the presence of LLJs, as explained in Marsham et al. (2011). We note that the position of the Saharan heat low in summer, as shown, e.g., in TCG16 (Figure 1) or in Lavaysse et al. (2013) (Figure 3), well coincides with the main zone of blue coloring of Figure 4. Four reasons may explain why the negative difference features (blue-colored) appears less in phase with Figure 8c of TCG16 than the positive difference features (orange-colored). First, the timing of the IASI observations is more favorable to the detection of LLJ peaking in the midmorning; second, the CALIOP vertical resolution is higher than that of IASI; third, the performance of CALIOP is less good in daytime; and fourth, the time periods analyzed are different but long enough to have only a marginal effect. It must, however, be recognized that, in particular due to the lack of in situ observations (see, e.g., Pantillon et al., 2016), it remains problematic to understand the reasons for differences between diurnal estimates of emission in various studies.

Next we compare the DEI diurnal differences with a proxy for dust emission, the Dust Uplift Potential (DUP) derived from surface wind observations during at most 5 months (May to September) of the year 2011 (see Roberts et al., 2018, for details) at three Automatic Weather Station (AWS) sites from the Fennec field campaign (Hobby et al., 2013), namely, F-101 (at the BBM supersite), F-134, and F-138, shown in Figure 4 (labels). At sites F-134 and F-138, morning DUP exceeds nighttime DUP indicative of the dominant LLJ mechanism, and confirmed by DEI: at both sites the climatological morning/nighttime DEI ratio is of ~2.7. In Figure 4 these sites lie in the blue colors indicating dominant morning emission. At site F-101, morning DUP still exceeds nighttime but the difference is less pronounced suggesting a greater contribution from haboobs (see Allen et al., 2013; Marsham, Hobby, et al., 2013). Again, this is confirmed by the DEI with a ratio of ~1.8. Although limited in time and spatial extent, these site observations give us confidence in the pan-Sahara DEI (Figure 3) and associated DEI diurnal difference (Figure 4). This comparison is, however, hampered by the difference in the definition of DEI and DUP, even if both tend to evaluate the emission intensity. In particular, the DUP depends on the surface wind speed through a threshold value triggering emission (Marticorena & Bergametti, 1995).

Finally, we can consider in more detail the Bodele depression, perhaps the best-known example of the role of morning LLJ dust emission (Washington & Todd, 2005). Our results in Figure 3a for the summer months only show strong emission very precisely from the location of the paleolake deposits (centered on ~17°N, 17°E) and, in Figures 3b and 4, show dominant nighttime emission. This latter result appears counterintuitive with a LLJ emission mechanism, despite being consistent with those of TCG16. This apparent issue can be resolved when considering the DEI diurnal difference over the whole year (Figure 5). This reveals that summer, and essentially the months of July and August (not shown), is the only season during which nighttime DEI is larger than morning DEI. In summer, haboob systems are most prevalent in the region likely associated with a marked evening peak in convection and rainfall in the region (Vizy & Cook, 2018).

During the rest of the year, in seasons 1 (DJF), 2 (MAM), and 4 (SON), DEI values of Bodele are higher in the morning than at nighttime, consistent with extensive previous work highlighting the morning peak in LLJ-driven dust emission, e.g., Washington and Todd (2005). Note that in winter months at night (Figure 5) high DEI values are observed around 13°E, 15°N, i.e., downwind of the Bodele paleolake. We infer that this represents the location of dust plumes emitted from the Bodele paleolake in the morning and subsequently transported at low levels, given the consistency of wintertime emission and transport in the Harmattan northeasterlies (Koren et al., 2006). On this evidence it seems that the DEI cannot easily distinguish fresh and recently transported dust during cooler winter months when the boundary layer is shallow and dust plumes remain in the near surface layers.

The Bodele DEI variability shown on Figure 6 can be compared to that of a region west of the Adrar des Ifoghas massif considered as the "hotspot" of emission in the Saharan heat low region (see Figure 3a and Ashpole & Washington, 2013). This region is different in its diurnal cycle due to the difference in the dominant dust uplift mechanisms acting at these two sites (Kocha et al., 2013), both regions being characterized by high dust emission, essentially in summer for Adrar des Ifoghas, almost all year round for Bodele.

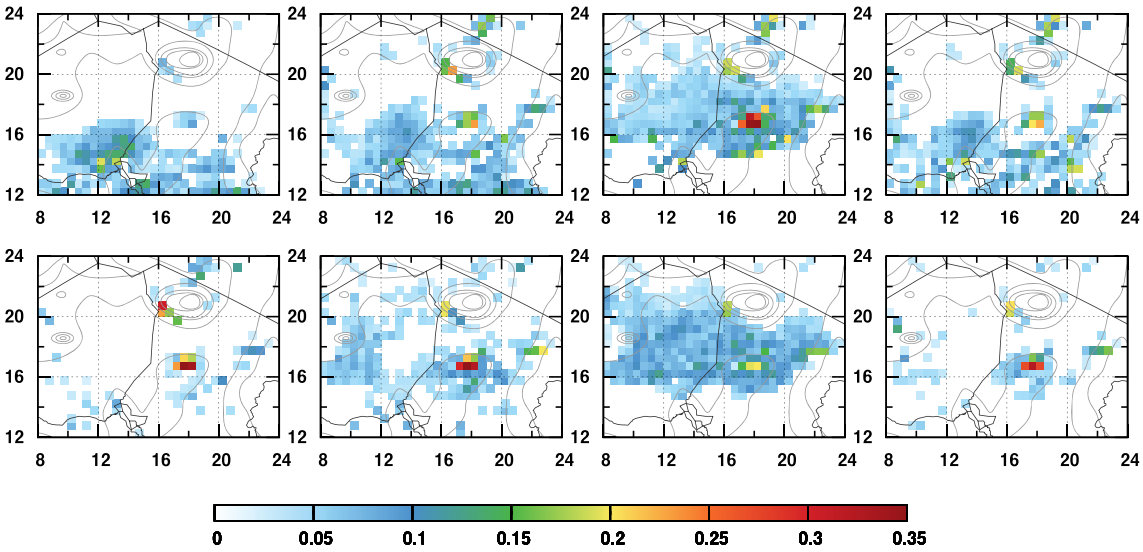

Figure 5. Seasonal IASI-DEI over a region centered on the Bodele. (top) Nighttime, (bottom) morning; from left to right: season 1 (DJF) to 4 (SON).

Figure 6 shows the DEI monthly climatology (July 2007 to December 2018) for Bodele (left), Adrar (right), morning in red and nighttime in blue. As expected, in summer, the Adrar region shows dominant nighttime emission when it is the opposite for Bodele, consistent with existing understanding (Knippertz & Todd, 2012). Indeed, for the region of Adrar, summer emissions are in general stronger at nighttime than morning presumably a reflection of haboob activity from moist convection in the evening; for the region of Bodele, morning emissions are stronger than nighttime ones due to the breakdown of the nocturnal LLJ, except in summer, essentially July and August, again due to moist convection as already seen (Figure 5; Vizy & Cook, 2018). Figure 7 presents, for the two regions Bodele (top) and Adrar (bottom) and the two main seasons of summer (JAS, left) and winter (DJF, right), interannual variations over the period 2007–2018. For Bodele, the difference between these two seasons is quite large, with larger nighttime DEI occurring in summer and the reverse in winter, as expected from Figure 6. For Adrar, larger summer nighttime DEI is also observed, but winter DEI is relatively small and their difference negligible. This figure highlights year-to-year DEI variability for both regions. For example, in summer 2007 and 2009, Adrar nighttime and morning DEIs are approximately equal due to the month of July for which the DEI is much larger morning than nighttime, something quite rare (not shown). For Bodele, an "anomaly" is seen in the summer of year 2016 with a sudden decrease of the nighttime DEI. This is due to a strong DEI maximum occurring in June and not in July or August. However, it is also seen that the DEI interannual variability is less important than the difference between morning and nighttime DEI. On Figure 7, one may also remark a slight positive trend in summer for both sites. However, the number of years considered is too small and cannot lead to a robust conclusion (Chedin et al., 2018).

Contrary to the two above results showing summer nighttime DEI dominating, the Fennec site F-134 (23.5°N, 0.3°W) shows a dominant summer morning DEI characteristic of morning LLJ (Hobby et al., 2013;

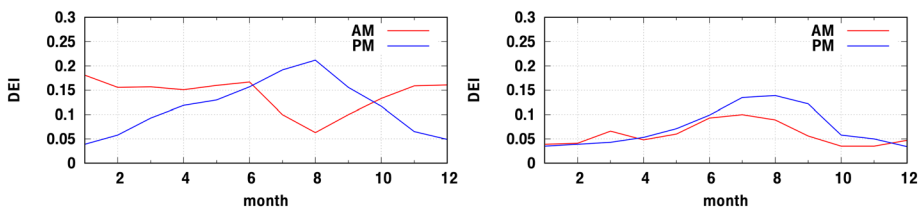

Figure 6. DEI 12-year average monthly climatology for Bodele centered at 17°N–18°E (±0.75, ±0.75) (left), and Adrar des Ifoghas centered at 19°N–1°E (±1.75, ±0.75) (right). Red curves = 0930 hr observations; blue curves = 2130 hr observations.

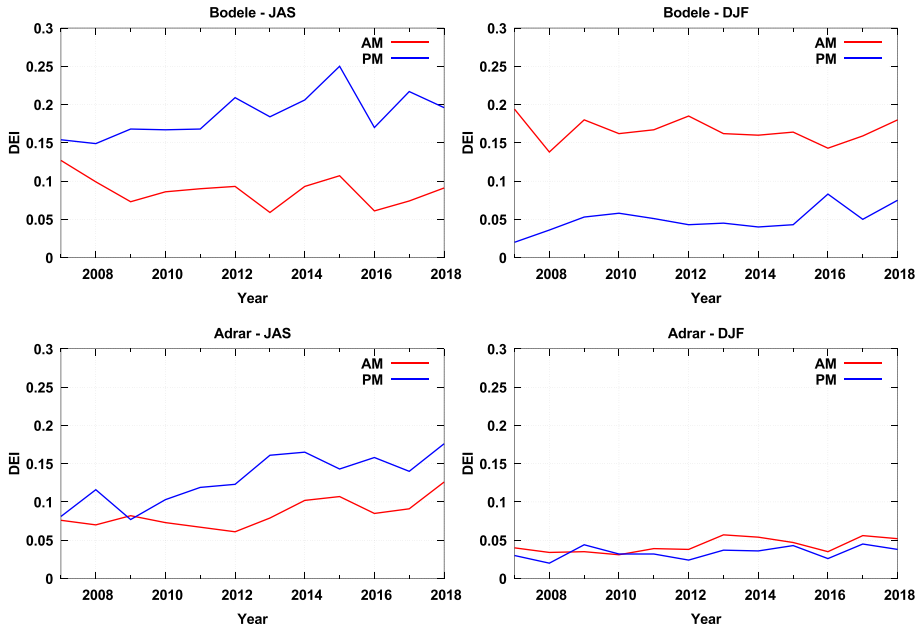

Figure 7. DEI interannual variations (2007–2018) for the two regions Bodele (top line) and Adrar des Ifoghas (bottom line) and the two seasons summer (JAS, left) and winter (DJF, right). Morning in red and nighttime in blue.

figure not shown). Here again, interannual variability is smaller than the mean difference morning minus nighttime DEI.

5. Conclusion and Caveats

Dust aerosols are an important component of the climate system. However, many issues remain unresolved and they continue to contribute one of the largest uncertainties to the total radiative forcing estimate (Boucher et al., 2013; Kok et al., 2017). The highly variable spatial and temporal distribution of dust aerosols including a pronounced diurnal cycle makes their study complex.

Here using an 11-year long time series (July 2007 to December 2018) of IASI-derived daily dust properties, dust AOD, and mean dust layer altitude (Capelle et al., 2018) at 0.5° resolution over Sahara, we have assessed the capability of IASI to bring limited but useful information on the dust diurnal cycle. IASI, crossing the equator at 0930 hr and 2130 hr local time, is relatively well matched with the times of occurrence of the main Saharan dust uplift mechanisms. In a first step, for each daily pixel, AOD-altitude bins have been classified into nine classes through the attribution of the category "High," "Medium," and "Low" to each of the two variables using predetermined threshold values. With the assumption that dust surface emission more corresponds to Low altitude-High AOD classes, we have compared, day-by-day, morning, and nighttime, our results to in situ Fennec June 2011 observations (Washington et al., 2012). Although such a comparison between space borne and in situ local observations is not trivial, conclusions are quite encouraging. An example for the 17th June (day and night) is given in this paper. In a second step, at climatological scale (2007–2011), regrouping the two classes Low altitude ($\leq$1.1 km asl) and High-Medium AOD ($\geq$0.5, i.e., about 1.0 in the visible), we have defined a DEI specific to IASI and analyzed its nighttime vs. morning differences over the whole Sahara as well as over more specific regions. Comparisons with already existing maps of dust sources (Ashpole & Washington, 2012, 2013; Formenti et al., 2011, 2014; Ginoux et al., 2012; Schepanski et al., 2007, 2009, 2012; Scheuvens et al., 2013; Weinzierl et al., 2017) or of alternate DEI (TCG16) show good agreement, globally (whole period) or seasonally. In summer, e.g., the peak dust season over Sahara, the impact of dust emission through the breakdown of the nocturnal low-level jet (NLLJ) associated with dust emissions peaking in the midmorning is well seen around the intense summertime Saharan heat low (Marsham et al., 2011). Similarly, nighttime DEIs larger than morning ones are seen for the regions of southern Algeria, northern Mali and northwest Niger, the regions west of the Aïr massif, or southern

Egypt-northern Sudan. There is evidence that these locations are preferred locations of haboobs (Allen et al., 2013; Knippertz et al., 2007; Marsham et al., 2008; Marsham, Dixon, et al., 2013; TCG16). This is also the case for the Bodele but only for the summer season and essentially the months of July and August suggesting that LLJ dominated in all months except high summer, consistent with understanding of the meteorology of the region (Vizy & Cook, 2018).

Several limitations of the method should be recognized. (i) Dust in the lowest atmospheric layer may not always be indicative of local emission. In winter, in particular but not only, dust plumes are often transported long distances in low atmospheric layers so that dust characterized by an altitude below 1.1 km and an infrared AOD larger than 0.5 (equivalent to 1 in the visible) may not represent local emission. As such the DEI is likely most accurate in summer months. (ii) In interpreting the physical mechanism behind the DEI diurnal difference, the assumption that morning DEI largely represents LLJ emission and nighttime DEI represents haboob emission may sometimes be a too limited framing. Convection and haboob activity occur over a broad diurnal window peaking in, but not limited to evening/nighttime hours and, moreover, haboobs can propagate for many hours after triggering within the MCS. (iii) IASI as any instrument has its advantages (global scale, measure of both AOD and altitude, equal quality of day and night observations, etc.); it also has its drawbacks: measuring at two precise times, it misses observation of prior or posterior daily dust events; close to the tropics, there are "holes" between two successive passes of the satellite (the present availability of IASI on board the METOP-B and METOP-C platforms could partly reduce this limitation). However, these limitations much less affect results at climatological scale. Moreover, the present IASI two snapshots instrument results have to be considered as a preliminary training phase for application to the at least hourly observations of the coming similar Infrared Sounder instrument (IRS), planned on board Meteosat Third Generation (2021).

The DEI from IASI complements previous analyses and contributes to an evolving picture of Saharan dust emission. Results of this study demonstrate the capability of IASI, on board the three platforms METOP-A, -B, and -C, to improve the documentation of dust distribution over Sahara over a long period of time. Associating observations of dust aerosols in the visible and in the infrared thus appears as a way to improve our knowledge of their impact on climate, its variability, and evolution.

Acknowledgments

This work has been supported in part by the European Space Agency (ESA) as part of the Climate Change Initiative Aerosol_CCI phase 2 project, by the Copernicus Climate Change Service (C3S), and by CNRS, CNES, and Ecole polytechnique. We have also benefited from the large facilities of IDRIS, the computer center of CNRS. We particularly acknowledge the EUMETSAT and EUMETCast service for providing IASI data and the AERIS data infrastructure for providing access to the IASI data (https://www.aeris-data.fr/). L2 retrieved AOD and altitude are available at https://iasi.aeris-data.fr/dust-aod_iasi_a_data/. We acknowledge the considerable efforts of the Fennec project in proving the observations of wind over the Sahara. Fennec was funded by a UK NERC consortium grant (NE/G017166/1). We are also grateful to the Reviewers and the Editor for their fruitful comments.

References

Allen, C. J. T., & Washington, R. (2014). The low-level jet dust emission mechanism in the central Sahara: Observations from Bordj-Badji Mokhtar during the June 2011 Fennec Intensive Observation Period. *Journal of Geophysical Research: Atmospheres*, *119*, 2990–3015. https://doi.org/10.1002/2013JD020594

Allen, C. J. T., Washington, R., & Engelstaedter, S. (2013). Dust emission and transport mechanisms in the central Sahara: Fennec ground-based observations from Bordj Badji Mokhtar, June 2011. *Journal of Geophysical Research: Atmospheres*, *118*, 6212–6232. https://doi.org/10.1002/jgrd.50534

Ansmann, A., Petzold, A., Kandler, K., Tegen, I., Wendisch, M., Muller, D., et al. (2011). Saharan Mineral Dust Experiments SAMUM-1 and SAMUM-2: What have we learned? *Tellus*, *63*(4), 403–429. https://doi.org/10.1111/j.1600-0889.2011.00555.x

Ashpole, I., & Washington, R. (2012). An automated dust detection using SEVIRI: A multiyear climatology of summertime dustiness in the central and western Sahara. *Journal of Geophysical Research*, *117*, D08202. https://doi.org/10.1029/2011JD016845

Ashpole, I., & Washington, R. (2013). A new high-resolution central and western Saharan summertime dust source map from automated satellite dust plume tracking. *Journal of Geophysical Research: Atmospheres*, *118*, 6981–6995. https://doi.org/10.1002/jgrd.50554

Bakker, N. L., Drake, N. A., & Bristow, C. S. (2019). Evaluating the relative importance of northern African mineral dust sources using remote sensing. *Atmospheric Chemistry and Physics*, *19*, 10525–10535. https://doi.org/10.5194/acp-19-10525-2019

Blackadar, A. K. (1957). Boundary layer wind maxima and their significance for the growth of nocturnal inversions. *Bulletin of the American Meteorological Society*, *38*(5), 283–290. https://doi.org/10.1175/1520-0477-38.5.283

Boucher, O., Randall, D., Artaxo, P., Bretherton, C., Feingold, G., Forster, P., et al. (2013). Clouds and aerosols. In T. F. Stocker, D. Qin, G.-K. Plattner, M. Tignor, S. K. Allen, J. Boschung, A. Nauels, Y. Xia, V. Bex, & P. M. Midgley (Eds.), *Climate Change 2013: The Physical Science Basis. Contribution of Working Group I to the Fifth Assessment Report of the Intergovernmental Panel on Climate Change*, edited by, (pp. 571–657). Cambridge, United Kingdom and New York, NY, USA: Cambridge University Press.

Callewaert, S., Vandenbussche, S., Kumps, N., Kylling, A., Shang, X., Komppula, M., et al. (2019). The mineral aerosol profiling from infrared radiances (MAPIR) algorithm: Version 4.1 description and evaluation. *Atmospheric Measurement Techniques*, *12*(7), 3673–3698. https://doi.org/10.5194/amt-12-3673-2019

Capelle, V., Chédin, A., Péquignot, E., Schluessel, P., Newman, S. M., & Scott, N. A. (2012). Infrared continental surface emissivity spectra and skin temperature retrieved from IASI observations over the tropics. *Journal of Applied Meteorology and Climatology*, *51*, 1164–1179. https://doi.org/10.1175/JAMC-D-11-0145.1

Capelle, V., Chédin, A., Pondrom, M., Crevoisier, C., Armante, R., Crépeau, L., & Scott, N. A. (2018). Infrared dust aerosol optical depth retrieved from IASI and comparison with AERONET over the period 2007–2016. *Remote Sensing of Environment*, *206*, 15–32. https://doi.org/10.1016/j.rse.2017.12.008

Capelle, V., Chédin, A., Siméon, M., Tsamalis, C., Pierangelo, C., Pondrom, M., et al. (2014). Evaluation of IASI derived dust aerosols characteristics over the tropical belt. *Atmospheric Chemistry and Physics*, *14*, 9343–9362. https://doi.org/10.5194/acp-14-9343-2014

Caquineau, S., Gaudichet, A., Gomes, L., & Legrand, M. (2002). Mineralogy of Saharan dust transported over northwestern tropical Atlantic Ocean in relation to source regions. *Journal of Geophysical Research*, *107*(D15), 4251. https://doi.org/10.1029/2000JD000247

Chalon, G., Cayla, F., & Diebel, D. (2001). IASI: An advanced sounder for operational meteorology, proceedings of the 52nd congress of IAF. (Oct. Toulouse France).

Chedin, A., Capelle, V., & Scott, N. A. (2018). Detection of IASI dust AOD trends over Sahara: How many years of data required? *Atmospheric Research*, *212*, 120–129. https://doi.org/10.1016/j.atmosres.2018.05.004

Clarisse, L., Clerbaux, C., Franco, B., Hadji-Lazaro, J., Whitburn, S., Kopp, A. K., et al. (2019). A decadal data set of global atmospheric dust retrieved from IASI satellite measurements. *Journal of Geophysical Research: Atmospheres*, *124*, 1618–1647. https://doi.org/10.1029/2018JD029701

Cowie, S. M., Knippertz, P., & Marsham, J. H. (2014). A climatology of dust emission events from northern Africa using long-term surface observations. *Atmospheric Chemistry and Physics*, *14*, 8579–8597. https://doi.org/10.5194/acp-14-8579-2014

Cuesta, J., Eremenko, M., Flamant, C., Dufour, G., Laurent, B., Bergametti, G., et al. (2015). Three-dimensional distribution of a major desert dust outbreak over East Asia in march 2008 derived from IASI satellite observations. *Journal of Geophysical Research: Atmospheres*, *120*, 7099–7127. https://doi.org/10.1002/2014JD022406

Damnati, B. (2000). Holocene lake records in the Northern Hemisphere of Africa. *Journal of African Earth Sciences*, *31*(2), 253–262. https://doi.org/10.1016/S0899-5362(00)00089-0

Emmel, C., Knippertz, P., & Schulz, O. (2010). Climatology of convective density currents in the southern foothills of the Atlas Mountains. *Journal of Geophysical Research*, *115*, D11115. https://doi.org/10.1029/2009JD012863

Engelstaedter, S., Tegen, I., & Washington, R. (2006). North African dust emissions and transport. *Earth-Science Reviews*, *79*, 73–100. https://doi.org/10.1016/j.earscirev.2006.06.004

Feuerstein, S., & Schepanski, K. (2019). Identification of dust sources in a Saharan dust hot-spot and their implementation in a dust-emission model. *Remote Sensing*, *11*, 4.

Flamant, C., Chaboureau, J. P., Parker, D. J., Taylor, C. M., Cammas, J. P., Bock, O., et al. (2007). Airborne observations of the impact of a convective system on the planetary boundary layer thermodynamics and aerosol distribution in the inter-tropical discontinuity region of the West African monsoon. *Quarterly Journal of the Royal Meteorological Society*, *133*, 1175–1189. https://doi.org/10.1002/qj.97

Flamant, C., Knippertz, P., Parker, D., Chaboureau, J.-P., Lavaysse, C., Agusti-Panareda, A., & Kergoat, L. (2009). The impact of a mesoscale convective system cold-pool on the northward propagation of the inter-tropical discontinuity over West Africa. *Quarterly Journal of the Royal Meteorological Society*, *135*(638), 139–159. https://doi.org/10.1002/qj.357

Formenti, P., Caquineau, S., Desboeufs, K., Klaver, A., Chevaillier, S., Journet, E., & Rajot, J.-L. (2014). Mapping the physico-chemical properties of mineral dust in western Africa: Mineralogical composition. *Atmospheric Chemistry and Physics*, *14*(19), 10663–10686. https://doi.org/10.5194/acp-14-10663-2014

Formenti, P., Schütz, L., Balkanski, Y., Desboeufs, K., Ebert, M., Kandler, K., et al. (2011). Recent progress in understanding physical and chemical properties of African and Asian mineral dust. *Atmospheric Chemistry and Physics*, *11*(16), 8231–8256. https://doi.org/10.5194/acp-11-8231-2011

Ginoux, P. J., Prospero, J. M., Gill, T. E., Hsu, N. C., & Zhao, M. (2012). Global-scale attribution of anthropogenic and natural dust sources and their emission rates based on MODIS Deep Blue aerosol products. *Reviews of Geophysics*, *50*, RG3005. https://doi.org/10.1029/2012RG000388

Gonzalez, L., & Briottet, X. (2017). North Africa and Saudi Arabia day/night sandstorm survey (NASCube). *Remote Sensing*, *9*, 896. https://doi.org/10.3390/rs9090896

Groß, S., Gasteiger, J., Freudenthaler, V., Müller, T., Sauer, D., Toledano, C., & Ansmann, A. (2016). Saharan dust contribution to the Caribbean summertime boundary layer—A lidar study during SALTRACE. *Atmospheric Chemistry and Physics*, *16*, 11535–11546. https://doi.org/10.5194/acp-16-11535-2016

Harrison, T. C., Washington, R., & Engelstaedter, S. (2019). A 14-year climatology of Saharan dust emission mechanisms inferred from automatically tracked plumes. *Journal of Geophysical Research: Atmospheres*, *124*, 9665–9690. https://doi.org/10.1029/2019JD030291

Heinold, B., Knippertz, P., Marsham, J. H., Fiedler, S., Dixon, N. S., Schepanski, K., et al. (2013). The role of deep convection and low-level jets for dust emission in summertime West Africa. *Journal of Geophysical Research: Atmospheres*, *118*, 4385–4400. https://doi.org/10.1002/jgrd.50402

Heintzenberg, J. (2009). The SAMUM-1 experiment over southern Morocco: Overview and introduction. *Tellus*, *61B*, 2–11. https://doi.org/10.1111/j.1600-0889.2008.00403.x

Hewison, T. J., Xiangqian, W., Fangfang, Y., Yoshihiko, T., Xiuqing, H., Dohyeong, K., & Koenig, M. (2013). GSICS inter-calibration of infrared channels of geostationary imagers using METOP/IASI. *IEEE Transactions on Geoscience and Remote Sensing*, *51*(3), 1160–1170. https://doi.org/10.1109/TGRS.2013.2238544

Hobby, M., Gascoyne, M., Marsham, J., Bart, M., Allen, C., Engelstaedter, S., et al. (2013). The Fennec automatic weather station n(AWS) etwork: Monitoring the Saharan climate system. *Journal of Atmospheric and Oceanic Technology*, *30*, 709–724. https://doi.org/10.1175/JTECH-D-12-00037.1

Holton, J. R. (1967). The diurnal boundary layer wind oscillation above sloping terrain. *Tellus*, *19*(2), 199–205. https://doi.org/10.1111/j.2153-3490.1967.tb01473.x

Klüser, L., Kleiber, P., Holzer-Popp, T., & Grassian, V. H. (2012). Desert dust observation from space—Application of measured mineral component infrared extinction spectra. *Atmospheric Environment*, *54*, 419–427. https://doi.org/10.1016/j.atmosenv.2012.02.011

Klüser, L., Martynenko, D., & Holzer-Popp, T. (2011). Thermal infrared remote sensing of mineral dust over land and ocean: A spectral SVD based retrieval approach for IASI. *Atmospheric Measurement Techniques*, *4*(5), 757–773. https://doi.org/10.5194/amt-4-757-2011

Knippertz, P., Deutscher, C., Kandler, K., Muller, T., Schulz, O., & Schultz, L. (2007). Dust mobilization due to density currents in the Atlas region: Observations from the Saharan Mineral Dust Experiment 2006 field campaign. *Journal of Geophysical Research*, *112*, D21109. https://doi.org/10.1029/2007JD008774

Knippertz, P., & Todd, M. C. (2010). The central west Saharan dust hot spot and its relation to African easterly waves and extratropical disturbances. *Journal of Geophysical Research*, *115*, D12117. https://doi.org/10.1029/2009JD012819

Knippertz, P., & Todd, M. C. (2012). Mineral dust aerosols over the Sahara: Meteorological controls on emission and transport and implications for modeling. *Reviews of Geophysics*, *50*, RG1007. https://doi.org/10.1029/2011RG000362

Kocha, C., Tulet, P., Lafore, J.-P., & Flamant, C. (2013). The importance of the diurnal cycle of Aerosol Optical Depth in West Africa. *Geophysical Research Letters*, *40*, 785–790. https://doi.org/10.1002/grl.50143

Kok, J. F., Ridley, D. A., Zhou, Q., Miller, R. L., Zhao, C., Heald, C. L., et al. (2017). Smaller desert dust cooling effect estimated from analysis of dust size and abundance. *Nature Geoscience*, *10*(4), 274–278. https://doi.org/10.1038/ngeo2912

Koren, I., Kaufman, Y. J., Washington, R., Todd, M. C., Rudich, Y., Martins, J. V., & Rosenfeld, D. (2006). The Bodele depression: A single spot in the Sahara that provides most of the mineral dust to the Amazon forest. *Environmental Research Letters*, *1*, 014005. https://doi.org/10.1088/1748-9326/1/1/014005

Kylling, A., Vandenbussche, S., Capelle, V., Cuesta, J., Klüser, L., Lelli, L., et al. (2018). Comparison of dust-layer heights from active and passive satellite sensors. *Atmospheric Measurement Techniques*, *11*, 2911–2936. https://doi.org/10.5194/amt-11-2911-2018

Lavaysse, C., Eymard, L., Flamant, C., Karbou, F., Mimouni, M., & Saci, A. (2013). Monitoring the West African heat low at seasonal and intra-seasonal timescales using AMSU-A sounder. *Atmospheric Science Letters*, *14*, 263–271. https://doi.org/10.1002/asl2.449

Lézine, A.-M., Bassinot, F., & Peterchmitt, J.-Y. (2014). Orbitally-induced changes of the Atlantic and Indian monsoons over the past 20,000 years: New insights based on the comparison of continental and marine records. *Bulletin de la Societe Geologique de France*, *185*(1), 3–12. https://doi.org/10.2113/gssgfbull.185.1.3

Liu, W., Cook, K., & Vizy, E. (2018). The role of mesoscale convective systems in the diurnal cycle of rainfall and its seasonality over sub-Saharan Northern Africa. *Climate Dynamics*, *52*(1-2), 729–745. https://doi.org/10.1007/s00382-018-4162-y

Marsham, J. H., Dixon, N., Garcia-Carreras, L., Lister, G. M. S., Parker, D. J., Knippertz, P., & Birch, C. E. (2013). The role of moist convection in the West African monsoon system—Insights from continental-scale convection-permitting simulations. *Geophysical Research Letters*, *40*, 1843–1849. https://doi.org/10.1002/grl.50347

Marsham, J. H., Hobby, M., Allen, C. J. T., Banks, J. R., Bart, M., Brooks, B. J., et al. (2013). Meteorology and dust in the central Sahara: Observations from Fennec supersite-1 during the June 2011 intensive observation period. *Journal of Geophysical Research: Atmospheres*, *118*, 4069–4089. https://doi.org/10.1002/jgrd.50211

Marsham, J. H., Knippertz, P., Dixon, N. S., Parker, D. J., & Lister, G. M. S. (2011). The importance of the representation of deep convection for modeled dust-generating winds over West Africa during summer. *Geophysical Research Letters*, *38*, L16803. https://doi.org/10.1029/2011GL048368

Marsham, J. H., Parker, D. J., Grams, C. M., Taylor, C. M., & Haywood, J. M. (2008). Uplift of Saharan dust south of the intertropical discontinuity. *Journal of Geophysical Research*, *113*, D21102. https://doi.org/10.1029/2008JD009844

Marticorena, B., & Bergametti, G. (1995). Modeling the atmospheric dust cycle: 1 Design of a soil-derived dust emission scheme. *Geophysical Research Letters*, *100*, 16415–16430. https://doi.org/10.1029/95JD00690

Pantillon, F., Knippertz, P., Marsham, J. H., Panitz, H.-J., & Bischoff-Gauss, I. (2016). Modeling haboob dust storms in large-scale weather and climate models. *Journal of Geophysical Research: Atmospheres*, *121*, 2090–2109. https://doi.org/10.1002/2015JD024349

Parker, D. J., Burton, R., Diongue, A., Ellis, R. J., Felton, M., Taylor, C. M., et al. (2005). The diurnal cycle of the west African monsoon circulation. *Quarterly Journal of the Royal Meteorological Society*, *131*(611), 2839–2860. https://doi.org/10.1256/qj.04.52

Pernin, J., Armante, R., Chedin, A., Crevoisier, C., Scott, N.A. (2013). Detection of clouds and aerosols over land and sea by day and night from hyperspectral observations in the thermal infrared, 3rd IASI Conference, Hyères, France, 4–8 Feb. Poster available at: http://ara.abct.lmd.polytechnique.fr

Peyridieu, S., Chédin, A., Capelle, V., Tsamalis, C., Pierangelo, C., Armante, R., et al. (2013). Characterization of dust aerosols in the infrared from IASI and comparison with PARASOL, MODIS, MISR, CALIOP, and AERONET observations. *Atmospheric Chemistry and Physics*, *13*, 6065–6082. https://doi.org/10.5194/acp-13-6065-2013

Peyridieu, S., Chédin, A., Tanré, D., Capelle, V., Pierangelo, C., Lamquin, N., & Armante, R. (2010). Saharan dust infrared optical depth and altitude retrieved from AIRS: A focus over North Atlantic—Comparison to MODIS and CALIPSO. *Atmospheric Chemistry and Physics*, *10*, 1953–1967. https://doi.org/10.5194/acp-10-1953-2010

Pierangelo, C., Chédin, A., Heilliette, S., Jacquinet-Husson, N., & Armante, R. (2004). Dust altitude and infrared optical depth from AIRS. *Atmospheric Chemistry and Physics*, *4*, 1813–1822. https://doi.org/10.5194/acp-4-1813-2004

Pierangelo, C., Mishchenko, M., Balkanski, Y., & Chédin, A. (2005). Retrieving the effective radius of Saharan dust coarse mode from AIRS. *Geophysical Research Letters*, *32*, L20813. https://doi.org/10.1029/2005GL023425

Roberts, A. J., & Knippertz, P. (2012). Haboobs: Convectively generated dust storms in West Africa. *Weather*, *67*(12), 311–316. https://doi.org/10.1002/wea.1968

Roberts, A. J., & Knippertz, P. (2014). The formation of a large summertime Saharan dust plume: Convective and synoptic scale analysis. *Journal of Geophysical Research: Atmospheres*, *119*, 1766–1785. https://doi.org/10.1002/2013JD020667

Roberts, A. J., Woodage, M. J., Marsham, J. H., Highwood, E. J., Ryder, C. L., McGinty, W., et al. (2018). Can explicit convection improve modelled dust in summertime West Africa? *Atmospheric Chemistry and Physics*, *18*, 9025–9048. https://doi.org/10.5194/acp-18-9025-2018

Ryder, C. L., McQuaid, J. B., Flamant, C., Rosenberg, P. D., Washington, R., Brindley, H. E., et al. (2015). Advances in understanding mineral dust and boundary layer processes over the Sahara from Fennec aircraft observations. *Atmospheric Chemistry and Physics*, *15*, 8479–8520. https://doi.org/10.5194/acp-15-8479-2015

Schepanski, K., Tegen, I., Laurent, B., Heinold, B., & Macke, A. (2007). A new Saharan dust source activation frequency map derived from MSG-SEVIRI IR-channels. *Geophysical Research Letters*, *34*, L18803. https://doi.org/10.1029/2007GL030168

Schepanski, K., Tegen, I., & Macke, A. (2012). Comparison of satellite based observations of Saharan dust source areas. *Remote Sensing of Environment*, *123*, 90–97. https://doi.org/10.1016/j.rse.2012.03.019

Schepanski, K., Tegen, I., Todd, M. C., Heinold, B., Bönisch, G., Laurent, B., & Macke, A. (2009). Meteorological processes forcing Saharan dust emission inferred from MSG-SEVIRI observations of sub-daily dust source activation and numerical models. *Journal of Geophysical Research*, *114*, D10201. https://doi.org/10.1029/2008JD010325

Scheuvens, D., Schütz, L., Kandler, K., Ebert, M., & Weinbruch, S. (2013). Bulk composition of northern African dust and ist source sediments—A compilation. *Earth Science Reviews*, *116*, 170–194. https://doi.org/10.1016/j.earscirev.2012.08.005

Tegen, I., Schepanski, K., & Heinold, B. (2013). Comparing two years of Saharan dust source activation obtained by regional modelling and satellite observations. *Atmospheric Chemistry and Physics*, *13*, 2381–2390. https://doi.org/10.5194/acp-13-2381-2013

Todd, M. C., Allen, C. J. T., Bart, M., Bechir, M., Bentefouet, J., Brooks, B. J., et al. (2013). Meteorological and dust aerosol conditions over the western Saharan region observed at Fennec Supersite-2 during the intensive observation period in June 2011. *Journal of Geophysical Research: Atmospheres*, *118*, 8426–8447. https://doi.org/10.1002/jgrd.50470

Todd, M. C., Bou Karam, D., Cavazos, C., Bouet, C., Heinold, B., Baldasano, J. M., et al. (2008). Quantifying uncertainty in estimates of mineral dust flux: An intercomparison of model performance over the Bodele Depression, northern Chad. *Journal of Geophysical Research*, *113*, D24107. https://doi.org/10.1029/2008JD010476

Todd, M. C., & Cavazos-Guerra, C. (2016). Dust aerosol emission over the Sahara during summertime from Cloud-Aerosol Lidar with Orthogonal Polarization (CALIOP) observations. *Atmospheric Environment*, *128*, 147–157. https://doi.org/10.1016/j.atmosenv.2015.12.037

Vizy, E. K., & Cook, K. H. (2018). Understanding the summertime diurnal cycle of precipitation over sub-Saharan West Africa: Regions with daytime rainfall peaks in the absence of significant topographic features. *Climate Dynamics*, *52*(5-6), 2903–2922. https://doi.org/10.1007/s00382-018-4315-z

Washington, R., Bouet, C., Cautenet, G., Mackenzie, E., Ashpole, I., Engelstaedter, S., et al. (2009). Dust as a tipping element: The Bodélé Depression, Chad. *Proceedings of the National Academy of Sciences of the United States of America*, *106*, 20564–20571.

Washington, R., Flamant, C., Parker, D. J., Marsham, J. H., McQuaid, J., Brindley, H., et al. (2012). Fennec—The Saharan climate system. *CLIVAR Exchanges*, *60*, 31–33.

Washington, R., & Todd, M. C. (2005). Atmospheric controls on mineral dust emission from the Bodélé Depression, Chad: The role of the low level jet. *Geophysical Research Letters*, *32*, L17701. https://doi.org/10.1029/2005GL023597

Washington, R., Todd, M. C., Engelstaedter, S., Mbainayel, S., & Mitchell, F. (2006). Dust and the low-level circulation over the Bodélé Depression, Chad: Observations from BoDEx 2005. *Journal of Geophysical Research*, *111*, D03201. https://doi.org/10.1029/2005JD006502

Weinzierl, B., Ansmann, A., Prospero, J. M., Althausen, D., Benker, N., Chouza, F., et al. (2017). The Saharan aerosol long-range transport and aerosol-cloud-interaction experiment: Overview and selected highlights. *Bulletin of the American Meteorological Society*, *98*(7), 1427–1451. https://doi.org/10.1175/BAMS-D-15-00142.1

Williams, E., Nathou, N., Hicks, E., Pontikis, C., Russel, B., Miller, M., & Bartholomew, M. J. (2009). The electrification of dust-lofting gust fronts ('haboobs') in the Sahel. *Atmospheric Research*, *91*, 292–298. https://doi.org/10.1016/j.atmosres.2008.05.017

Yu, H., Tan, Q., Chin, M., Remer, L. A., Kahn, R. A., Bian, H., et al. (2019). Estimates of African dust deposition along the trans-Atlantic transit using the decade long record of aerosol measurements from CALIOP, MODIS, MISR, and IASI. *Journal of Geophysical Research: Atmospheres*, *124*, 7975–7996. https://doi.org/10.1029/2019JD030574